# Enhancement of The Physical Properties of Electrospun Tubular Structure Nanofibers Produced From Low Concentration of Polyacrylonitrile Solution By Addition Boehmite Nanoparticles.

**Salih Abbas Habeeb[1], Laleh Rajabi[2], Farzad Dabirian[3]**

[1]Polymers and Petrochemical Industries Lab. Faculty of Materials Engineering,
University of Babylon, Hilla, Iraq, drsaleh.abbas@uobabylon.edu.iq , Mobile: +9647804671642
[2]Polymer Research Lab., Faculty of Petroleum and Chemical Engineering, Razi University, Kermanshah, Iran.
[3]Department of Textile Engineering, Faculty of Engineering, Razi University, Kermanshah, Iran.

**DOI : 25.10.2018/3rdchemconf_14**

**Abstract-** Polyacrylonitrile (PAN)/Boehmite nanofibrous composite tubular structures fabricated from dilute polymer solutions by typical electrospinning method. The specimen tested by X-ray diffraction, scanning electron microscopy, Fourier Transform Infrared Spectroscopy, Fast Fourier Transform method and tensile tests.Presence of boehmite nanoparticles in the electrospun PAN nanofibers prevented bead formation, resulted in uniform fibers with smaller diameters, and improved alignment from low concentration PAN polymer solutions. 0.6 wt. % boehmite-loaded nanofibrous composite tubular structure was selected as the optimum formulation to proceed with the crystallinity and tensile tests, which, showed enhanced the porosity and mean surface area and crystalline properties as well as an abrupt shift in tensile performance. Tensile properties of the nanofibers strongly depended on their crystalline properties. The strong intermolecular forces (hydrogen bonds) acting amidst the Al-OH collections at the surface of BNP and the polar CN groups along the polymer chains.

**Key Words:** Typical electrospinning; Tubular structure; Mean Surface Area; Boehmite Nanoparticles; Low Concentration.

## Introduction

Electrospinning considered the simplest and most effective technology to produce continuous polymer nanofibers from polymer solutions or melts in high electrical fields (Ren , 2013). The advantages embrace its relative ease, low cost, high speed, large materials choice, and flexibility. In addition, this method permits management over fiber diameter, microstructure, and arrangement [Homaeigohar et al, 2014]. It produces fibers with the high specific area and porosity levels(Dabirian andHosseini, 2009;Xie et al,2010;Wang et al,2014; Chen et al,2017)with diameters variable within the range of nano to the micrometer. Electrospun nanofibers from very different polymers employed in filters, composites, tissue-engineering scaffold, protecting cloth¬ing, electronics, catalysis, ceramic fibers, wound dressing, drug delivery materi¬als and different applications(Dabirian and Hosseini, 2009)
(Wang et al,2014). The properties classify the applications of the nanofibers, for example, reduction in dimension of nanofibers can lead to new properties, such as quantum effects, adsorption behavior, or catalytic selectivity(Shi et al,2015;Chen et al,2017). To fabricate fibers that are not only non-woven meshes but also aligned, patterned, twisted yarn, and three-dimensional structures, developing new methods for controlling the deposition behavior of the fibers either by mandrel collector shaft, rotating drums, disk collectors or parallel electrodes are required (Dabirian and Hosseini, 2009; Chen et al,2017).Electrospinning parameters classified into method parameters, solution parameters and close parameters (Panda, 2007;
Yener et al, 2012). The concentration of polymeric solution plays a vital role for delimited properties of the electrospun nanofibers (Beachley andWen, 2009).Extremely focused solutions permit manufacturing additional uniform fibers with fewer beads additionally the assembly of larger fiber diameters (Huang et al,2003; Mo et al,2004;Yang et al ,2004) (Bhardwaj and Kundu ,2010;Garg and Bowlin , 2011;Niu et al ,2011;Sreedhara et al,2013).The form of the beads additionally changes from spherical to spindle like once the polymer concentration will

increase. On the opposite hand, the rise of polymer concentration plays a vital role within the alignment of nanofibers that successively affects the mechanical properties (CHEN et al, 2006). Recent studies have shown that the alignment of nanofibers improved molecular orientation and, therefore, improved mechanical properties than the every which way oriented nanofibers (Sadrjahani et al, 2010;García-Moreno et al, 2017).The key parameters controlling the formation of fibers by electrospinning suchasthe solution viscosity is a vital parameter that influences the fiber size and morphology throughout electrospinning once the polymer solution stretched throughout electrospinning from the needle tip to the collector. The electrospun jet of low viscosity polymer solution breaks into small droplets or creates beaded fibers. The quantity of entanglements will increase with increasing the viscosity, resulting in uniform fibers with few beads and these entanglements stop the jet from breaking apart throughout the process (García-Moreno et al, 2017).Therefore, low concentration electrospinning solution produces a high quantity of beads, while highly concentrated solutions produce more uniform fibers with fewer beads (Mo et al,2004;Yang et al ,2004).However, with high concentration electrospinning solution the solidification rate increases, which leads to the retardation in the crystallization, process, thus, decreasing the glass transition temperature (Yang et al, 2004). On the other hand, the mechanical properties additionally found to be obsessed with fiber diameter. The fibers with a smaller diameter had a better strength, however, lower malleability because of the upper draw quantitative relation that applied throughout the electrospinning method (Chronakis, 2005;Chae et al, 2006; Sreedhara and Tata, 2013).Polymer nanofibers can be continuous and have high mechanical properties especially at the production of the nanofibrous tubular scaffolds with oriented nanofibers (Wu et al, 2010).PAN nanofiber could be a common precursor of general carbon fibers. However, these applications of PAN nanofibers restricted by the poor strength, because of their small diameters and low molecular orientation and crystallinity within the fibers (Song et al, 2011). However, reinforcement of these nanofibers with organic or inorganic nanoparticles may lead to tremendous improvement in fiber quality.The advantage of using nanoparticles is to add a second phase that dispersed within the matrix and has nanoscale dimensions, the small size of which leads to unique properties (Lin et al,2009;Mohamad and Kong, 2010). Enhanced fiber quality by reducing fiber diameter and bead formation because of adding nanoparticles in the polymeric matrix reported by (Saquing et al, 2009;Jin et al, 2017). Direct fabrication of three-dimensional flower-like (carbon nanotube) CNT nanofiber foams by freeze-drying of binary compound solutions of electrospun PAN nanofibers and CNTs to supply multiple bedded CNT nanosheets with large enough surface area and wonderful mechanical properties and adsorption capacities for selective adsorption processes and environmental applications. (Sun et al, 2016) created polyacrylonitrile (PAN)/γ-AlOOH electrospun composite nanofibers for top adsorption of heavy metals. (Zhang et al, 2008)produced boehmite nanofibers by nanoparticles assembly without a surfactant, the composite nanofibers having a high specific surface area and slender pore-size distribution. (Kuiry et al, 2005)mentioned the formation mechanism of the boehmite nanofibers discriminatory growth on the longitudinal axis because of the interaction inter alia the solvent molecules, therefore, the surface OH teams of the boehmite nanoparticles through hydrogen bonding. Boehmite nanoparticles area unit high potential multi radical compounds. The centers of boehmite structure include paired layers of octahedral for metallic element ions; therefore, the layers themselves are imperturbable of octahedral chains. The part of fully crystallized BNP contains a blocky orthorhombic structure (Rajabiand Derakhshan, 2010). Currently, the tubular fibrous structures generally created by manually rolling up a nanofibrous membrane or by precipitation of nanofibers on a rotating metal or Teflon rod go-ahead by the elimination of the rod collector. However, these ways are unable to retain the alignment consistency or uniformity of the overlaid fibers (Jana and Zhang, 2013).

The aim of work manufacting a composite tubular structures from dilute polymer solutions by the opposite charge electrospinning method and studying the effect of the presence of boehmite nanoparticles (BNP) on bead formation, fiber diameter, continuity and alignment which in turn could affect the crystalline as well as tensile properties of the fabricated nanofibers that, constructed the nanofibrous tubular structures. Boehmite nanoparticles used as high potential multi hydroxyl compound that could interact with PAN as the main constructing polymer material of the nanofibers and thus, affect the properties of the resulting nanofibrous composite tubular structures.

**Materials and methods**

**Materials**

Commercial Polyacrylonitrile (PAN) powder with the molecular weight of a hundred (g/mol) was equipped by Poly Acryl Company, Iran. N, N-Dimethylformamide (DMF, 99.5%)obtained fromMerck (Schuchardt OHG 85662 Hchenbrunn, Germany).Boehmite nanoparticles [aluminum oxide hydroxide (γ-AlO-OH)] was synthesized with the particle size (30-35 nm) and OH/Al ratio (3.5), from aluminum nitrate [(Al ($NO_3$)] and sodium hydroxide (NaOH), buy from Merk, based on the method reported earlier (Rajabiand Derakhshan ,2010).

**Electrospinning and Preparation of the Nanocomposite Polymer Solutions**

Table 1 presents the electrospinning conditions and the polymer solution compositions for the production of nanofibrous composite tubular structures through typical charge electrospinning method.

Table1. The electrospinning conditions and polymer solution compositions.

| Electrospinning conditions | PAN / BNP ( wt.% ) |
|---|---|
| The distance between needle and collector 15 cm | 10:0.0 |
| Solution feed rate of 0.6 mL/hr. | 10:0.3 |
| The rotational speed of mandrel collector 2164 rpm. | 10:0.6 |
| The applied voltage between two opposite needles 16 kV | 10:0.9 |
| PAN Concentration 10 wt.% | 10:1.2 |

To prepare each nanocomposite polymer solution, the appropriate amounts of the corresponding nanoparticle and solvent (DMF) were mixed. The mixture sonicated in an ultrasonic bath (240 w-35 kHz, SONEX Digit C Ultrasonic bath, DT52 H model made by the Bandelin Company, Germany) for 10 min at ambient temperature. Then, the appropriate amount of PAN powder was added to the sonicated mixture which was further stirred on a magnetic stirrer for 3 hr below 30ºC to obtain a homogeneous polymer solution, keeping the amount of solvent unchanged. At last, the nanocomposite polymer solution was sonicated for another 10 min to finally ensure the dispersion of the nanoparticles in the mixture and to obtain a well-mixed homogeneous nanocomposite polymer solution mixture, ready to proceed for electrospinning. **Fig.1** shows the preparation steps of the nanocomposite polymer solutions schematically and theelectrospinning set-up included a direct current (DC) power supply, a high voltage transformer, asyringe with metallic needle, metal mandrel collector and a high voltage transformer betweena syringe pump and mandrel collector.

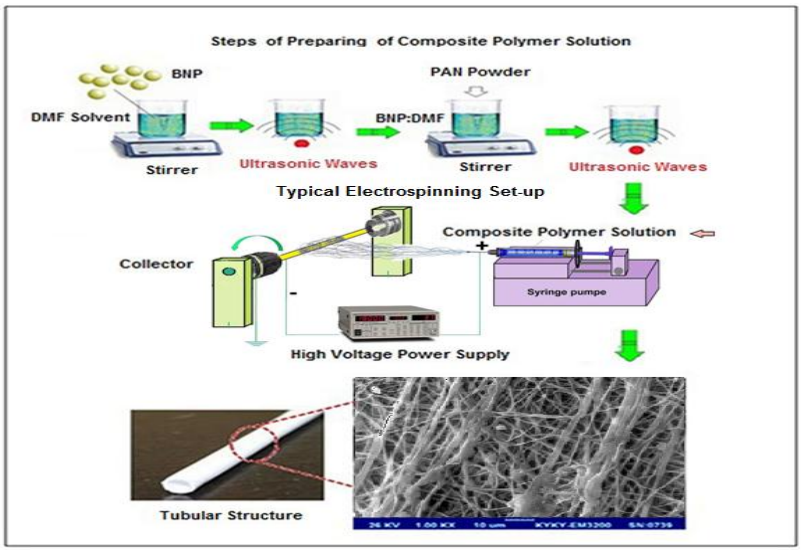


**Fig.1** Schematic diagram for preparation steps of the nanocomposite polymer solutions and electrospinning set-up.

**Morphological**

Morphology of the collected fibers discovered beneath Associate in Nursing environmental scanning electron microscopy (SEM), KYKY–EM 3200 model, the surface of samples were coated with a layer of gold with the thickness of 100 Å by using the sputter coater KYKY-SBC12. The average diameter with standard deviation (St.Dev.) calculated using the Digitizer image analysis software program and QI Macros (SPC Software for Excel, Six Sigma Software) plotted the frequency histograms of nanofibers diameter distribution. The morphology of the boehmite nanoparticles examined by transmission electron microscopy (TEM, Philips CM10, high tension, 100 kV).

**Alignment of composite nanofibers.**

Fast Fourier Transform (FFT) method utilized to distinguish the feasible groups and vibrational modes of the materials as well as to quantify the alignment of nanofibers.

Images were processed with (SPIP-TM) (version 6.7.4)image metrology(A/ S)( Hørsholm, Denmark software analysis) (Scanning Probe Image Processor ) transform to 8-bit SEM image from white color to black with the (TIF files) had dimensions(256 × 256 or 512 × 512) pixels.for used one Fourier analysis, the FFT high resolution function (Requires the Extended Fourier or Calibration Module) , which means that the profile will be mean value padded so that it contains 16 times more elements before calculating its Fourier transform.

For theFFT/PSD testapplied to calculate the fast Fourier transform and power spectrum density with two – dimension calculated as the power value normalized with the area size of each element. PSD(u ,v) = P(u ,v) / ( x Domain *y Domain) …where x Domain and y Domain are physical ranges of the source image and (u ,v) are u ,v the discrete Fourier indexes =0,1,2 .

**Mechanical Properties**

Tensile properties of the nanofibrous tubular structures obtained by the Universal Testing Machine (UTM), [Hi-Zwick model 1446-60, the samples were prepared according to the ASTM D-638-14 standard (2.0 cm in length, mounted on the clamps to be tested at the speed of 5 mm/min until the sample broke).

**Fourier Transformed Infrared Spectroscopy**

Orderly for distinguishing the chemical structure moreover, infrared spectroscopy of the composite the Fourier Transform Infrared Spectroscopy (FTIR), Bruker-ALPHA, Germany, in the range of 400-4000 $cm^{-1}$with a resolution of 2 $cm^{-1}$ and 64 scans used for characterization.

**X-Ray Diffraction**

The structural and morphological characterizations of the composite nanofiber structures were performed by X-ray diffraction (XRD), Philips PAN analytical: X'Pert Pro MPD X-ray diffractometer at room temperature using X-Ray Tube: Cu (Kα= 1.54 Å), Generator Settings: 40 mA, at 40 kV and 2θ = 3º-40º, Step Size [°2Th.]: 0.0260.

**Surface Areas and Porosity of Nanofibers Analysis**

There are a little procedures for checking the porosity such as image analysis (Sreedhara and Tata, 2013) byusing images were processed with SPIP(TM) version (6.7.4). Image metrology A/S , Hørsholm , Denmark software analysis (Scanning Probe Image Processor ) (Catena et al ,2016) to detect the pores in the SEM image and calculated the porosity (%), mean surface area $(nm)^2$ ± standard deviation, mean pores diameter (nm) ± standard deviation and the heights intensity(Y%) of distribution pores using the threshold method according to the following:

1- Limited the inspection box on the surface of the image

2- Detected the diameter of the mean pores with standard deviation (Std. Dev.) and surface area with (Std. Dev.) on the surface of the image

3- Plotted the histogram with limited the heights intensity of pores distribution(Y %)and porosity%

## 3. Results and Discussion

**Effect of BNP on Morphological Properties of theNanofibrous Composite Tubular Structures**

**Fig. 2** shows the TEM photograph of the produced BNP, who is the orthorhombic structure with mean particle size of 30 nm detected.

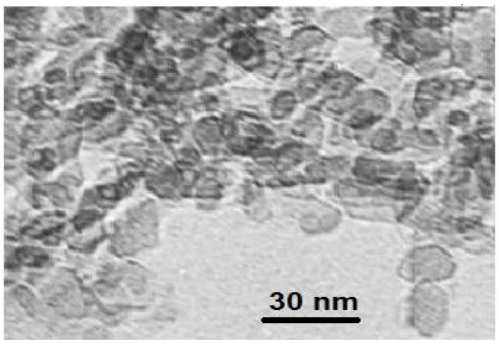


**Fig. 2** TEM image of boehmite nanoparticles.

The boehmite containing nanofibers produced by the typical electrospinning method under the conditions given in **Table 1**. A low polymer solution concentration studied in order that scrutinize the influence of the corresponding nanoparticles on the uniformity and continuity of the nanofibrous composites produced from dilute polymer solutions through electrospinning. **Fig.3** shows the SEM micrographs, 3D topographical micrograph acquired by SPIP imaging sftware and histogram diameter distribution of the nanofibers with and without boehmite nanoparticles.

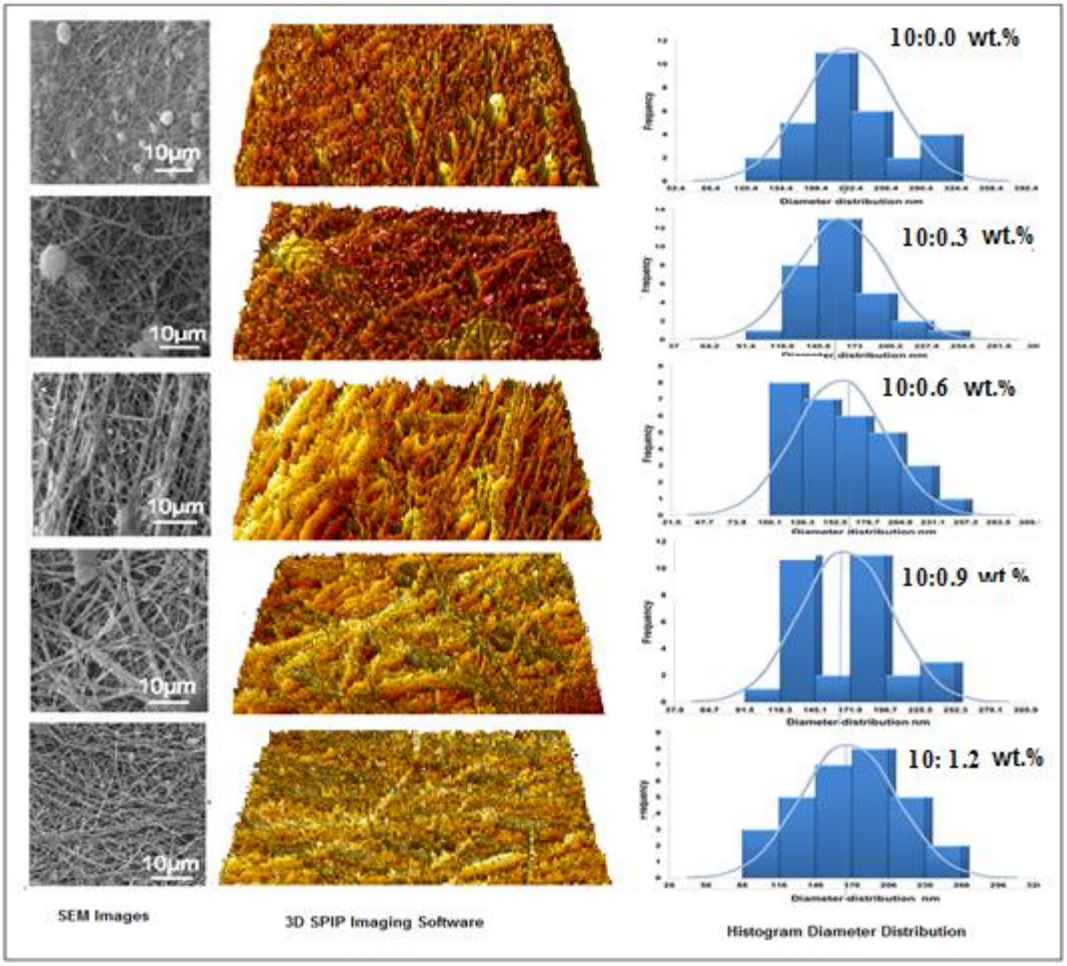


**Fig. 3** SEM micrographs, 3D topographical micrograph acquired by SPIP imaging softwareand frequency histogram of nanofibers diameter distribution of the nanofibrous composite structures.

Presence of boehmite nanoparticles effect of the bead formation by decreasing both the number and the size of the beads throughout the structure of the nanofibrous composites, also after transformed the SEM images into 3D micrographs by used image processing software SPIP(Tahalyani et al ,2018) .We noted that, the change the beads numbers,shapes and improve the surface morphology of composite nano fibers with the increasing theloading of BNP.

The average diameter, standard deviation (Std.Dev)and the diameter range of nanofibers decreased from 210.25±40.05 nm to 166.3±39.17 nm in addition the range decreasing from 130-280 nm to90-222 nm respectively. According to increasing the loading of BNP from the until 0.6 wt.%, whereas, the average diameter increased from 178.8±35.71 nm to 183.27±49.08 nm and the range of nan fibers diameter increased from 124-258 nm to 114-264 nm for the formulations loaded with BNP higher than 0.6 wt.%

Boehmite nanoparticles having a multi hydroxyl compounds that can interface together with the amine groups of the PAN through H-O, which may significantly affect the ability to move the polymer chains lead to potential bonding between the particles and the polymer and bridging of the polymer chains. **Fig. 4** shows the potential hydrogen bonding between boehmite nanoparticles and CN side groups along the polymer chains (CN...HO-Al).

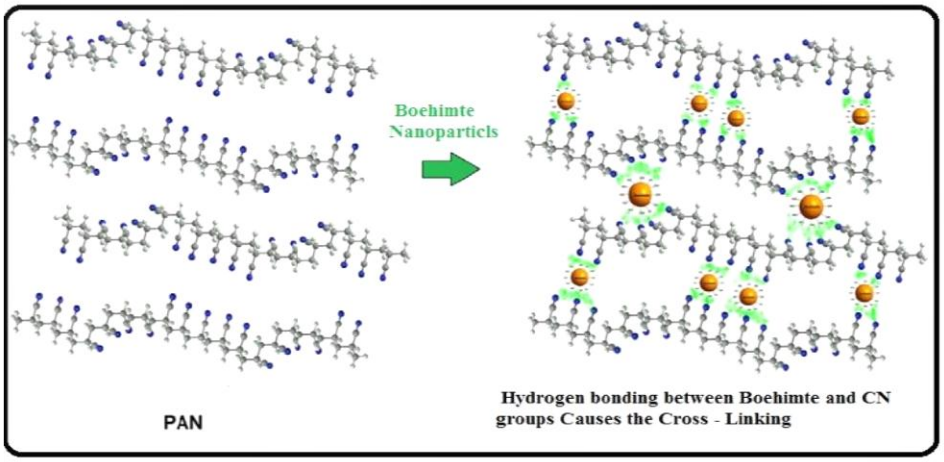


**Fig. 4** Potential intermolecular forces (H-O) between the BNP and CN side groups of PAN along the polymer chains (CN..OH-AL).

Thismay be responsible for the morphological alterations that observed lead to the existence of the BNP in the structure of the nanofibrous composites. However, Increasing the amount of boehmite increased the chances of agglomeration of the nanoparticles and thus, decreased the homogeneity in the electrospinning polymer solution, that influenced in transition the morphological properties of the boehmite-loaded nanofiber structures above 0.6 wt.%.Agglomeration of nanoparticles can also affect the extent of interactions between the amine groups of the polymer and the boehmite nanoparticle crystals.Therefore,the lower amounts of nanoparticles lead to unique properties. The 0.6 wt.% boehmite containing nanofibers produced the best results as they contained the least number as well the smallest size of beads in their structure, these results have been reported by other researchers as well (Zhang et al ,2008;Yeom et al ,2010) .

**Effect of BNP on Alignment of the Nanofibrous Composites**

**Fig.5** presents the SEM micrographs, FFT high-resolution curves, and 2D FFT / PSD analysis,the FFT alignment of the nanofibrous composite structures loaded with various amounts of boehmite nanoparticles produced by the typical electrospinning method. The FFT analysis of the SEM images of the nanofibrous. Composite samples were used to characterize the anisotropy of the scaffolds to digitize the alignment level of the nanofibers, the FFT values multiplied from 2.917 to 5.141, once multiplied the loading of BNP till 0.6 wt.% and reduced the FFT values to 3.716, once multiplied the loading of BNP quite 0.6 wt.% . Conjointly at the 2D FFT / PSD, the floral grayscale pixels were distributed within the output image of the FFT analysis image to mirror the degree of fiber alignment of the initial information image, such analysis technique has been reported by different researchers still (Kim et al ,2016;Lai et al ,2011). The FFT knowledge of pictures of the photographs} with aligned nanofibers resulted in output images with non-randomly and elliptically distributed pixels. The element intensities premeditated between zero to 360°, and the degree of alignment within the FFT information mirrored the form and height of the height. In addition, the upper the intensity and fewer occurrences of peaks indicated that the alignment of the nanofibers was highly ordered as presented in **Fig. 5**.

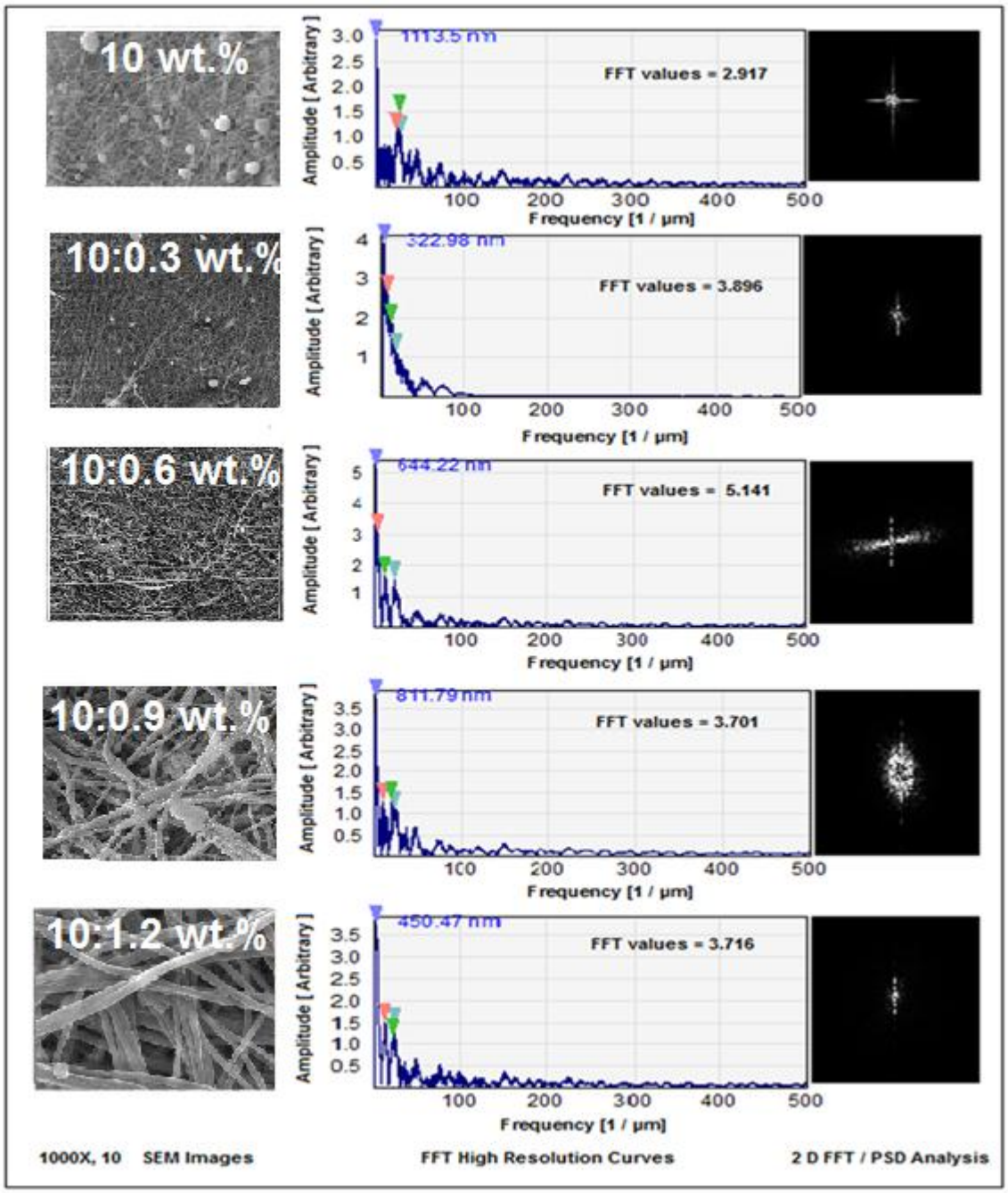


**Fig .5** The SEM images, FFT high-resolution curves and 2D FFT / PSD analysis of composite nanofibers after loading the BNP.

**Effect of BNP on TensileProperties of Nanofibrous Composites**

These set of experiments were also performed on the boehmite loaded nanofibrous composites containing four different amounts of nanoparticles (0.3, 0.6, 0.9 and 1.2 wt.%), keeping all other electrospinning parameters constant. Presence of the boehmite nanoparticles in lower amounts positively affected the tensile properties of the nanofibers as given in **Table 2**.Elastic modulus increased from 48.58cN/tex for the reference nanofibers without any boehmite content to 58.92 and 67.06cN/tex for the 0.3 and 0.6 wt. % BNP loaded nanofibers. However, it decreased significantly on further increasing the number of nanoparticles to 0.9 and 1.2 wt.%, which can be attributed tomore chances of nanoparticle agglomeration with higher amounts of nanoparticles and thus,converting the electrospinning polymeric solution towards non-homogeneity. On the other hand, the elongation at break decreased from7.93% for the reference

nanofibers without any boehmite content to (6.35 and 6.52) for the 0.3 and 0.6 wt. % boehmite-loaded nanofibrous composites at low filling the nanoparticles could be deal regularly across the substrate of polymer matrix . For high filling, yonder is the inclination for the fibers to groups jointly and hence limit the improvement of the mechanical characteristicsthe high loading due to an increase in brittleness and weak inter-phase bonding between polymer matrix and the boehmite fiber (Mohamad and Kong, 2010).

Table 2. Tensile parameters of pure PAN and the boehmite loaded nanofibrous composite structures.

| PAN / BNP ( wt.% ) | Max. load ( N ) | Stress ( cN / tex ) | E- Mod. ( cN / tex ) | Elongation at break (% ) |
|---|---|---|---|---|
| 10.00 | 5.73 | 3.25 | 48.58 | 7.93 |
| 10: 0.3 | 6.94 | 3.52 | 58.92 | 6.35 |
| 10: 0.6 | 10.72 | 5.67 | 67.06 | 6.52 |
| 9: 0.9 | 4.41 | 2.27 | 29.20 | 7.13 |
| 9: 1.2 | 5.82 | 3.87 | 32.30 | 8.25 |

**FTIR analysis of the nanofibrous composites**

Fig.6 shows the FTIR spectra of pure boehmite nanoparticles, pure PAN nanofibers, and the PAN/BNP (0.6wt.%) nanofibrous composite as it proved to be the best composition among the formulations studied. The absorption bands at the frequencies of 3448.27 and1072.69 $cm^{-1}$ in the FTIR spectrum of boehmite nanoparticles corresponded to the elongated indecision of OH bonded to Al. The absorption bands at the frequencies of 1072.69 $cm^{-1}$ were associated with the symmetrical bending vibrations of H bonds OH….OH, and therefore the ones at the frequencies 735, 635.3 and 484.69 $cm^{-1}$ additionally named AL-O vibration modes, that are in sensible agreement with those reported within the literature (Zhang et al ,2008). For pure PAN nanofibers the absorption peak at 2244 $cm^{-1}$ associated with the stretching vibration of C≡N and also the absorption peaks within the regions 2870-2944, 1450-1460, 1350-1380 and 1220-1270 $cm^{-1}$ associated with the various vibrational modes of C-H within the aliphatic teams (CH and CH2) on the PAN chains. The addition of boehmite nanoparticles to PAN-led to the looks of recent peaks in PAN/BNP (0.6 wt.%) spectrum associated with the boehmite vibration modes. The 3 peaks at 784.95, 628.88 and 490.84 $cm^{-1}$ associated with the vibration modes of Al-O-Al in BNP. The peak at the frequency of 1086.74 $cm^{-1}$ associated with the vibration of H bonding between Al-OH groups as also reported by other researchers(Lin et al ,2009;Sun et al ,2016;Ghezelgheshlaghi et al ,2017).

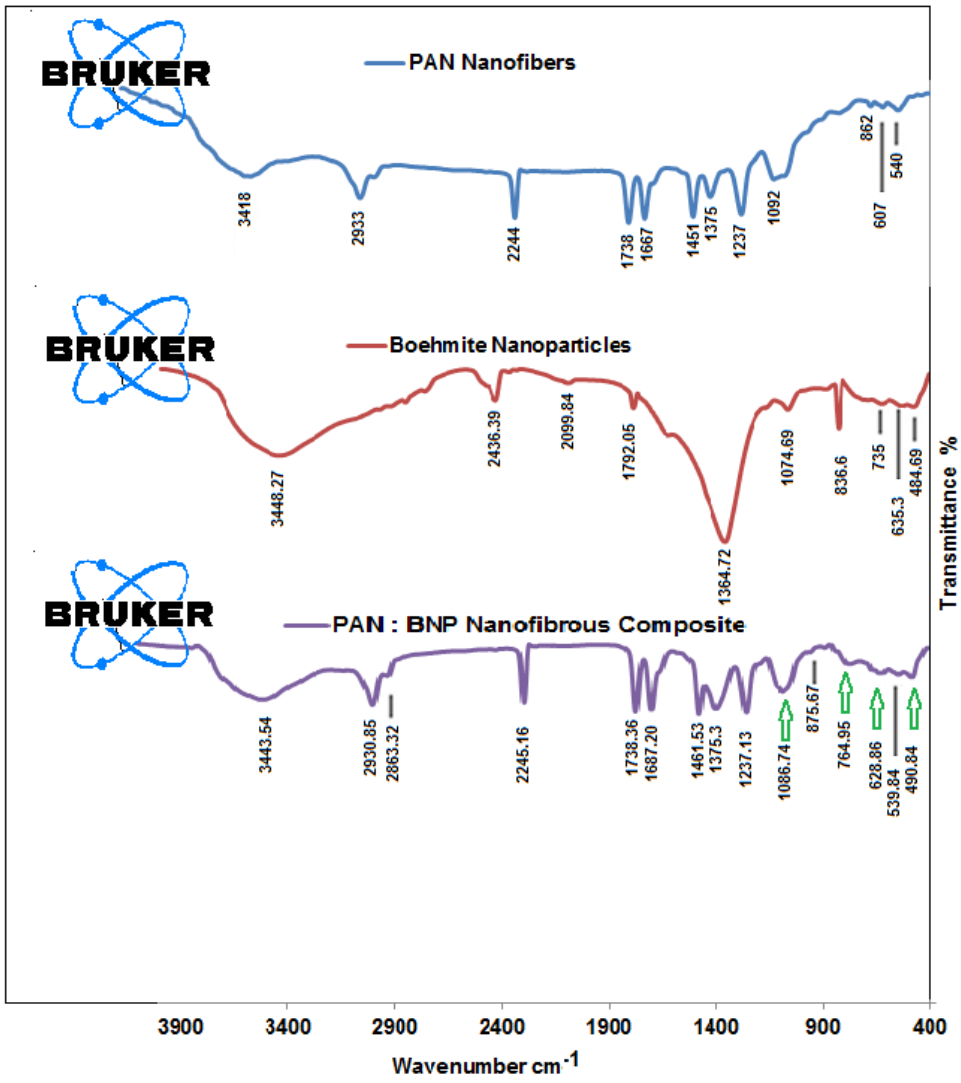


**Fig. 6** FTIR spectra of BNP, PAN nanofibers and (10:0.6 wt. %) PAN/BNP nanofibrous composite

**Effect of BNP on Crystallinity of Nanofibrous Composites**

X-rays penetrate into the solid non-destructively and provide information about the inner structure of solids. Crystal acts as a natural diffraction grating for the diffraction of X-ray beam incident upon it in all directions. The X-rays diffracted in accordance with the Bragg's law.

$n\lambda = 2d\ sin\,\theta.$ (1)

$D = \frac{K\lambda}{\beta}\cos\theta$(2)

Where 'n' is an integer explain to the order of reflexing, 'λ' is that the wavelength, 'd' is that the spacing between the crystal lattice planes responding for explicit diffracted beam and 'θ' is that the angle that incident beam makes with lattice planes. The width of the Bragg's reflection during a normal X-ray powder diffraction pattern will give the data of the common grain size. The peak growth will increase with decreasing the grain size exploitation Scherer's relation in step with equation (2) evaluates the common crystal size.

wherever 'λ' is that the X-ray wavelength, 'β' is that the full width at half most of diffraction peak, 'θ' is that the diffraction angle and 'K' is that the Scherer's constant of the order of unity for usual crystal (Bindu and Thomas, 2014;Gaber et al ,2014).In addition,$\lambda$ =1.54Å and K=0.90, $\beta$ = *FWHM* at reflection intensity 100% (Song et al, 2011).The degree of orientation Π (%) can be estimated by using the totally polished azimuthal density allocation diffracted of the

(100) reflexing at d-spacing [Å]. The degree of orientation calculated by the following equation.

$$\Pi = \frac{180° - \Delta\varphi^{\frac{1}{2}}}{180°} \quad (3)$$

Where Δφ 1/2 symbolize the FWHM of the azimuthally scanned peak and the φ symbolize the corrected (χ) azimuthal angles between the distortion direction and the normal direction of personage a crystal planes. This angle calculated by the equations:

$$(\chi) \ = \theta - FWHM \quad (4)$$

$$cos\,\varphi = cos\,\chi\, cos\,\theta \quad \text{(Murthy, 2016)} \quad (5)$$

Crystallinity is usually calculated as a magnitude relation of the diffraction part of the crystal a part of the tubular structure specimen (Ic) in addition of the overall diffraction from an equivalent specimen, I(c+ b). The amounts of Ic will be acquired when an acceptable subtraction of the scattering part from the background, Ib.

$C\% = \left(\frac{Ic}{I}\right)$ 100% (6) Aanywhere: I total = I (c + b) (Alemdar and Sain , 2008;Song et al, 2011). In the X'Pert Pro system, the measuring of the crystallinity (%) was achieved by the described of crystalline (peak zone) and amorphous zone (background zone) on a scope acquired from the examined material. The software system integrated all pixels inside the "peak zone" in addition as all pixels within the "background zone" to get the values for I + Ib within the on top of an equation. The background in those sizes was estimated as a second-order polynomial method also was automatically ablated of the full density of the "peak zone" to get Ic. The "peak zone" and therefore the "background zone" held steady during tubular structure specimens. **Fig. 7** presents the (XRD) patterns of the pure PAN nanofibrous tubular structure (10.0 wt. %) which of 0.6 wt. % BNP-loaded nanofibrous composite. The nanofibers were orienting on the winding direction of the rotating mandrel collector. The peaks at 2θ ≈ 17.2° and 2θ ≈ 29.6° are public to the fiber diffraction model of PAN by hexangular packing as also reported by other researchers (Jalili et al ,2006).Moreover, the XRD peak at 2θ ≈ 26.7° countsforthe nanofibrous composite. Table 3 presents the values of the degree of orientation, the average crystallite size and percent crystallinity for PAN nanofibers and the nanofibrous composite. All the three properties enhanced due to the presence of BNP. Considering both, the tensile and crystallinity properties of the nanofibrous structures, it observed that they strongly affected mutually. It has also been reported by (Song et al,2011), that, the fibers with improved in PAN crystals and higher polymer molecular orientation lead to improving the mechanical properties.Production of bead-free nanofibers is unavoidable with low concentration polymer solutions. However, the presence of boehmite nanoparticles in the electrospun PAN nanofibers prevented bead formation and resulted in uniform fibers from low concentration PAN polymer solution.Presence of boehmite nanoparticles in an appropriate amountalso decreased fiber diameter with respect to pure PAN nanofibers.Nanofibers better aligned in the nanofibrous composite structures. In addition, the BNP-loaded nanofibrous compositesexhibitedenhanced crystalline properties as well as an abrupt shift in tensile performance, which in turn was strongly depended on their crystalline properties.

**Table 3.** The degree of orientation, crystallite size, and crystallinity of the pure PAN nanofibers and the nanofibrous composite structures.

| Samples | Degree of orientation (%) | Average crystallite size (nm) | Crystallinity (%) |
|---|---|---|---|
| 10.0 wt.% PAN | 56.3 | 5.87 | 30.78 |
| 10:0.6 wt.% PAN:BNP | 65.1 | 7.6 | 52.45 |

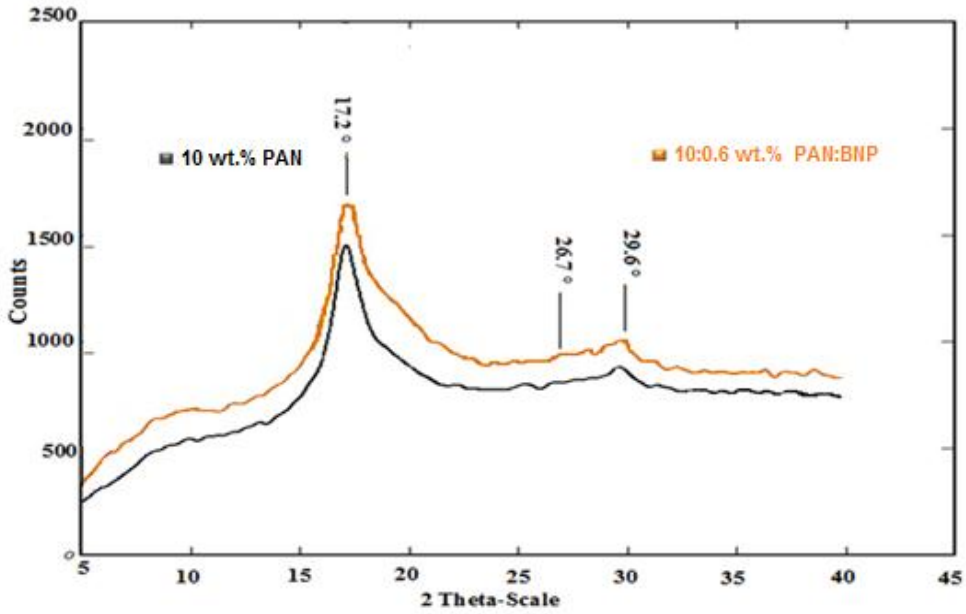


**Fig. 7** XRD patterns of PAN nanofibers and the 0.6 wt. % boehmite-loaded nanofibrous composite.

**Effect of the BNP on Porosity and Surface Area of Composite Nanofibers.**

**Figure 8** and **Table 4**, show the effect of BNP on porosity (%) , mean surface area( nm)$^2$ with standard deviation (Std. Dev.), mean pores diameter with standard deviation(Std. Dev.) (nm ) and height intensity (Y%) of pores distribution of tubular strictures nanofibrous by using the threshold method to detect the Pores in the SEM images with SPIP software analysis .

The change in the pores size not normally distributed by using the Kruskal-Wallis test (XLSTAT Analysis Software, 2016 for Microsoft Excel versions) (one-way ANOVA). The data reported about the changes in mean pore size ± (Std. Dev) statistical significance accepted at $P > 0.05$ for increased the loading of BNP. Therefore, when increased the loading of BNP until 0.6 wt. %, the percentage of the heightened intensity of pores distribution, percentage porosity and the mean surface area increased. Also, decreased the diameter of the mean pores and slightly increased the particles size distribution of BNP in the web of composite nanofibers ( **Fig. 8, Table 4**), the best porosity(%), surface area (nm$^2$) and highest intensity of distribution pores at 0.6 wt. %. On the others hand, decreased the porosity (%), the mean surface area (nm)$^2$ and height intensity (Y %) of distribution pores on histogram curves with increased the loading of BNP more than 0.6 wt.% and increased the mean pore size ± (Std. Dev). Therefore, we noted that the composite nanofibers web containing the heights surface area with lowest pores size and pores diameter distributionbecome narrower with the lowest loading of BNP(Zhang et al ,2008;Mohamad and Kong ,2010;Alphonse and Faure , 2013).

**Table 4** The results of porosity (%), mean surface area, mean pores diameter and height intensity of pores distribution (Y%) and particles size (nm) by SPIP image processing software by using the threshold method after increased the loading of BNP into the low polymer solution.

| Samples | Porosity % | SurfaceArea nm$^2$ | Pores Size nm | Particles Size nm |
|---|---|---|---|---|
| 10:0.0 | 39.12 | 1469.072±159.7 | 10.67±1.4 | - |
| 10: 0.3 | 44.5 | 3984.87±154.74 | 8.9±1.67 | 5.83±2.40 |
| 10: 0.6 | 47.28 | 49700.17±108.07 | 3.6±1.70 | 5.313±0.45 |
| 10: 0.9 | 44.23 | 19685.01±161.8 | 6.67±1.97 | 4.88 ±0.50 |
| 10: 1.2 | 43.76 | 5679.23± 108.5 | 6.75±1.4 | 4.75 ±0.53 |

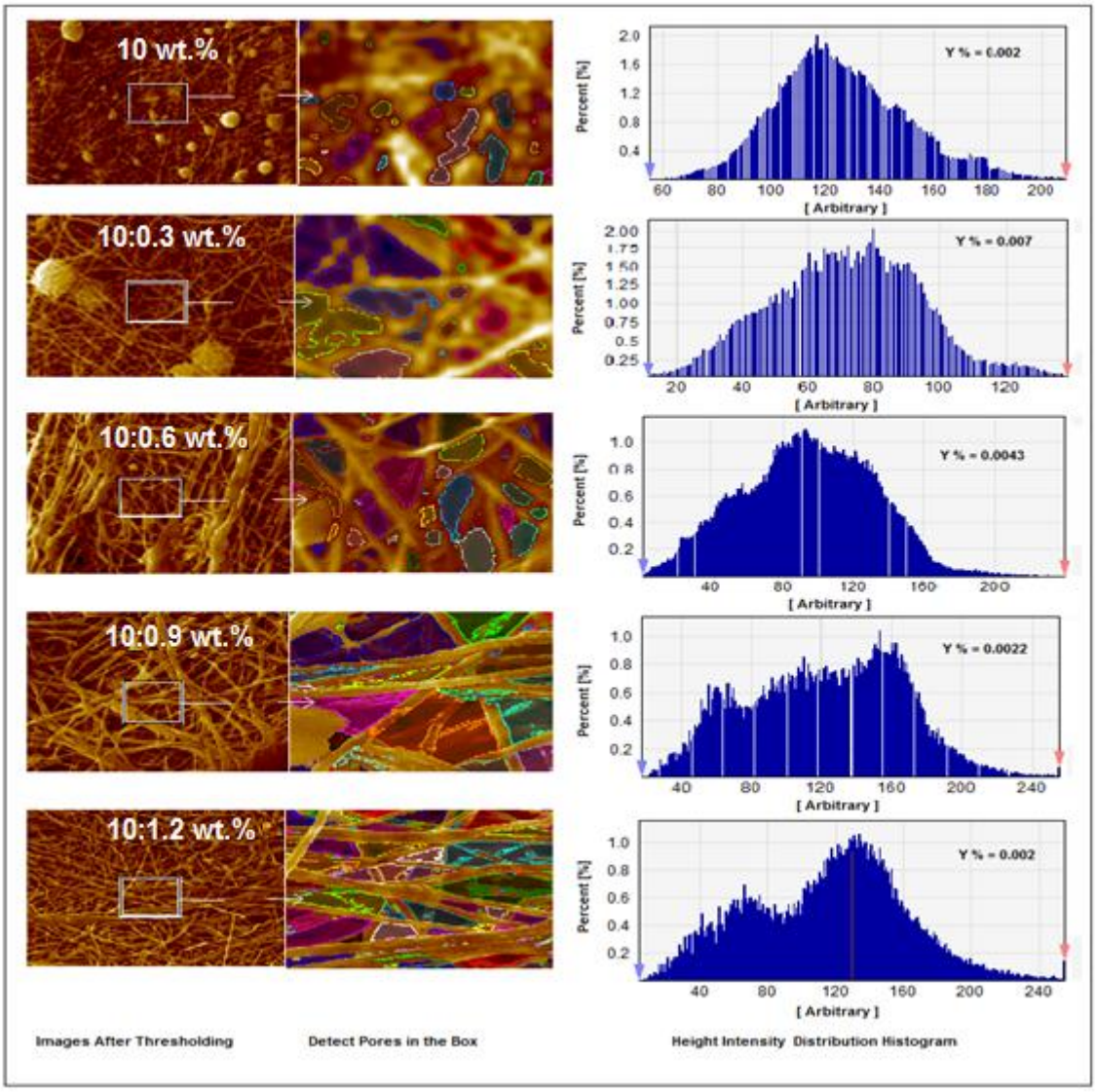


**Fig .8** SEM micrographs after thresholding, detected pores and height intensity histogram analysis of the nanofibers without any BNP and with loading BNP.

## CONCLUSIONS

Bead-free continuous and aligned PAN/boehmite nanofibrous composite tubular structures fabricated from dilute polymer solutions by typical electrospinning method. The 0.6wt. % boehmite containing nanofibrous structures had the least number as well the smallest size of beads in their structure. The average diameter and the diameter range of nanofibers decreased as a result of the presence of boehmite nanoparticles up to 0.6 wt.% which were inversely affected by higher amounts of nanoparticles. The presence as well as increasing the amounts of nanoparticles increased the alignment of the nanofibers until the 0.6 wt.% BNP-loaded PAN nanofibrous composite was selected as the best formulation, which exhibited enhanced crystalline properties, porosity, mean surface area as well as an abrupt shift in tensile performance. Tensile properties of the nanofibers strongly depended on their crystalline properties, porosity and surface area. Hence, the presence of boehmite nanoparticles in an appropriate amount imposed a balance in controlling the instability of electrospun jet deposition at low polymer concentrationelectrospinning solution that, lead to decreasing the number of beads and achieving considerable enhancement of the nanofibrous composite tubular

structure properties such as continuity, alignment, crystallinity, porosity , mean surface area and tensile properties.

**REFERENCES**

Alemdar, A and M.Sain (2008). 'Isolation and characterization of nanofibers from agricultural residues–Wheat straw and soy hulls.' Bioresour Technol 99(6):1664-71

Alphonse, P and B. Faure (2013). "Synthesis of highly porous alumina-based materials." Microporous Mesoporous Mater 181:23-28.

Beachley, V and X.Wen (2009). "Effect of electrospinning parameters on the nanofiber diameter and length." Mater. Sci. Eng. C 29(3):663-668.

Bhardwaj, N and S.C.Kundu (2010). "Electrospinning: a fascinating fiber fabrication technique." Biotechnol. Adv 28(3):325-347.

Bindu, P and S.Thomas (2014). "Estimation of lattice strain in ZnO nanoparticles: X-ray peak profile analysis." Journal of Theoretical and Applied Physics 8(4):123-134.

Chronakis, I.S (2005). 'Novel nanocomposites and nanoceramics based on polymer nanofibers using electrospinning process—a review." J. Mater. Process. Technol 167(2-3):283-293.

Chae, H.J, M.L.Minus and S.Kumar (2006). 'Oriented and exfoliated single-wall carbon nanotubes in polyacrylonitrile." Polymer 47 (10):3494-3504.

Chen, M,P.K. Patra ,S.B. Warner and S. Bhowmick (2006). "Optimization of electrospinning process parameters for tissue engineering scaffolds." Biophys. Rev. Lett 1(02):153-178

Catena,A,Q. Guo Q,M.R. Kunze, S.Agnello,F.M. Gelardi, S.Wehner and C.B.Fischer (2016). "Morphological and chemical evolution of gradually deposited diamond-like carbon films on polyethylene terephthalate: from subplantation processes to structural reorganization by intrinsic stress release phenomena." ACS Appl. Mater. Interfaces 8(16):10636-10646

Chen, J, Q.Niu, G.Chen,J. Nie and G.Ma (2017). "Electrooxidation of Methanol on Pt@ Ni Bimetallic Catalyst Supported on Porous Carbon Nan fibers." J. Phys. Chem. C 121(3): 1463-1471

Dabirian, F and S. Hosseini (2009). "Novel method for nanofibre yarn production using two differently charged nozzles." Fibres Text. East. Eur 17(3): 45-47.

Fennessey, S.F and R.J. Farris (2004). "Fabrication of aligned and molecularly oriented electrospun polyacrylonitrile nanofibers and the mechanical behavior of their twisted yarns." Polymer 45(12):4217-4225.

Garg, K and G.L.Bowlin (2011)."Electrospinning jets, and nanofibrous structures." Biomicrofluidics 5(1): 013403

Gaber, A, M.A.Abdel-Rahim, A.Y.Abdel-Latief and M.N.Abdel-Salam (2014). "Influence of calcination temperature on the structure and porosity of nanocrystalline SnO2 synthesized by a conventional precipitation method." Int J Electrochem Sci. 9(1):81-95

García-Moreno, P.J,N. Özdemir, K.Stephansen , R.V. Mateiu,Y. Echegoyen,J.M. Lagaron, I.S.Chronakis and C.Jacobsen (2017). "Development of carbohydrate-based nano-microstructures loaded with fish oil by using electrohydrodynamic processing." Food Hydrocoll 69:273-285

Ghezelgheshlaghi, S, M.R. Mehrnia,M. Homayoonfal and M.M. Montazer-Rahmati (2017). 'Al2O3/poly acrylonitrile nanocomposite membrane: from engineering design of pores to efficient biological macromolecules separation." J. Porous Mater:1-21.

Huang, Z.M.,Y.Z. Zhang, M.Kotaki andS.A.Ramakrishna (2003). "Review on polymer nanofibers by electrospinning and their applications in nanocomposites." Compos. Sci. Technol 63(15):2223-2253

Homaeigohar, S and M. Elbahri (2014). Nanocomposite electrospun nanofiber membranes for environmental remediation. Materials 7(2):1017-1045.

Jalili, R, M.Morshed and S.A.Ravandi (2006). "Fundamental parameters affecting electrospinning of PAN nanofibers as uniaxially aligned fibers." J. Appl. Polym. Sci 101(6):4350-4357

Jana, S and M. Zhang (2013). "Fabrication of 3D aligned nanofibrous tubes by direct electrospinning." J. Mater. Chem. B 1(20):2575-2581.

Jin, L,B. Hu, S.Kuddannaya, Y.Zhang,C. Li and Z. Wang (2017). "A three-dimensional carbon nanotube–nanofiber composite foam for selective adsorption of oils and organic liquids.' Polym. Compos. DOI:10.1002/pc.24334

Kuiry, S.C,E. Megen, S.D.Patil,S.A. Deshpande and S. Seal (2005). "Solution-based chemical synthesis of boehmite nanofibers and alumina nanorods." J. Phys. Chem. B 109(9):3868-3872.

Kim, J.I,T.I Hwang, L.E.Aguilar, C.H.Park and C.S. Kim (2016). "A Controlled Design of Aligned and Random Nanofibers for 3D Bi-functionalized Nerve Conduits Fabricated via a Novel Electrospinning Set-up." Sci. Rep. 6 23761; DOI: 10.1038/srep 23761.

Lin, N, G.Chen, J.Huang,A. Dufresne and P.R.Chang (2009). "Effects of polymer-grafted natural nanocrystals on the structure and mechanical properties of poly (lactic acid): A case of cellulose whisker-graft-polycaprolactone." J. Appl. Polym. Sci 113(5):3417-3425

Lai, E.S, C.M.Anderson and G.G.Fuller (2011). "Designing a tubular matrix of oriented collagen fibrils for tissue engineering." Acta Biomater 7(6):2448-2456.

Mo, X.M., C.Y.Xu, M.F.Kotaki and S. Ramakrishna (2004). "Electrospun P (LLA-CL) nanofiber: a biomimetic extracellular matrix for smooth muscle cell and endothelial cell proliferation." Biomaterials25(10):1883-1890 .

Mohamad, R. N and Y.L.Kong (2010). "Synthesis of Alumina Nanofibers and Composites." . In: Ashok Kumar (Ed.). Nanofibers, InTech; 2010. p. 406-418

Murthy,N.S(2016) ."X-ray Diffraction from Polymers."In: Qipeng GUO, (ED). Polymer Morphology: Principles, Characterization, and Processing.Hoboken, NewJersey: John Wiley &Sons.INC,p. 14-36.

Niu, H, X.Wang and T. Lin(2011)."Needleless electrospinning: developments and performances". In: Dr. Tong Lin (Ed.). Nanofibers-Production, Properties and Functional Applications. InTech; 2011. P. 17-36

Panda, P.K(2007). "Ceramic nanofibers by electrospinning technique—A review." T INDIAN CERAM SOC 66(2):65-76.

Rajabi, Land A.A. Derakhshan (2010). "Room temperature synthesis of boehmite and crystallization of nanoparticles: effect of concentration and ultrasound." Sci Adv Mater 2(2):163-172

Ren, C(2013). "PAN Nanofibers and Nanofiber Reinforced Composites." ( M.S. Thesis) University of Nebraska-Lincoln. https://digitalcommons.unl.edu/mechengdiss/59/

Saquing, C.D, J.L. Manasco and S.A. Khan (2009). "Electrospun nanoparticle–nanofiber composites via a one-step synthesis.' Small 5(8):944-951.

Sadrjahani, M, S.A.Hoseini, V.Mottaghitalab,A.K. Haghi (2010). "Development and characterization of the highly oriented pan nanofiber." Braz. J. Chem. Eng 27(4):583-589

Song, Z, X.Hou, L. Zhang and S. Wu (2011). "Enhancing crystallinity and orientation by hot-stretching to improve the mechanical properties of electrospun partially aligned polyacrylonitrile (PAN) nanocomposites." Materials 4(4):621-632.

Sreedhara, S.S and N.R.Tata (2013). "A novel method for measurement of porosity in nanofiber mat using pycnometer infiltration." J Eng Fiber Fabr 8:132-137.

Shi, Q, Y.Lei, Y.Wang, H.Wang, L.Jiang, H.Yuan, D.Fang, B.Wang,N. Wu and Y.B.Gou (2015). "N-codoped 3D micro-/mesoporous carbon nanofibers web as efficient metal-free catalysts for oxygen reduction." Curr. Appl. Phys 15(12):1606-1614.

Sun,B, X.Li, R. Zhao, M.Yin, Z.Wang, Z. Jiang and C. Wang (2016). "Hierarchical aminated PAN/γ–AlOOH electrospun composite nanofibers and their heavy metal ion adsorption performance." J Taiwan Inst Chem Eng 62:219-227

Tahalyani, J , S.Datar and K.Balasubramanian (2018). "Investigation of dielectric properties of the free-standing electrospun nonwoven mat." J. Appl. Polym. Sci. 135(16):46121.

Wu, H,J. Fan ,C.C. Chu and J. Wu (2010). 'Electrospinning of small diameter 3-D nanofibrous tubular scaffolds with controllable nanofiber orientations for vascular grafts." J. Mater. Sci. Mater. Med 21(12):3207-3215.

Wang, S.H.,Y. Wan, B. Sun,L.Z. Liu andW. Xu (2014). "Mechanical and electrical properties of electrospun PVDF/MWCNT ultrafine fibers using a rotating collector." Nanoscale Res. Lett 9(1):522.

Xie, J, M.R.MacEwan, A.G. Schwartz and Y. Xia (2010). "Electrospun nanofibers for neural tissue engineering." Nanoscale 2(1): 35-44 .

Yang, F, C.Y.Xu, M.Kotaki , S.Wang and S. Ramakrishna (2004). "Characterization of neural stem cells on electrospun poly (L-lactic acid) nanofibrous scaffold." J. Biomater. Sci., Polym. Ed 15(12):1483-1497

Yeom, B.Y, E.Shim and B. Pourdeyhimi (2010). "Boehmite nanoparticles incorporated electrospun nylon-6 nanofiber web for new electret filter media." Macromol Res 18(9):884-90.

Yener ,F, O.Jirsak and R.Gemci (2012). "Using a range of PVB spinning solution to acquire diverse morphology for electrospun nanofibres." Iran. J. Chem. Chem. Eng. (IJCCE) 31(4):49-58.

Zhang, J, F.Shi, J.Lin, S.Y.Wei, D.Chen, J.M.Gao, Z.Huang,X.X. Ding and C.Tang C(2008). 'Nanoparticles assembly of boehmite nanofibers without a surfactant. Mater. Res." Bull 43(7):1709-15.